Computers and Mathematics with Applications 71 (2016) 238–254

Contents lists available at ScienceDirect

Computers and Mathematics with Applications

journal homepage: www.elsevier.com/locate/camwa

Efficient numerical schemes for fractional water wave models

Can Li [a,b,*], Shan Zhao [b,c]

[a] Department of Applied Mathematics, School of Sciences, Xi'an University of Technology, Xi'an, Shaanxi 710054, PR China
[b] Beijing Computational Science Research Center, Beijing 100084, PR China
[c] Department of Mathematics, University of Alabama, Tuscaloosa, AL 35487, USA

ARTICLE INFO

Article history:
Received 20 June 2015
Received in revised form 11 October 2015
Accepted 14 November 2015
Available online 3 December 2015

Keywords:
Fractional water wave models
Finite difference schemes
Stability
Convergence

ABSTRACT

In this paper, efficient numerical schemes are proposed for solving the fractional water wave models that describe the propagation of surface water wave. By using the weighted and shifted Grünwald–Letnikov (WSGL) formula to approximate the nonlocal fractional operators, we design a series of second order accurate difference schemes for the considered models. The existence, stability and convergence of numerical solutions of the proposed numerical schemes are established rigorously. The analysis shows that the proposed numerical schemes are unconditionally stable with second order accuracy for both temporal and spatial discretizations. Several numerical results are provided to verify the efficiency and accuracy of our theoretical analysis.

1. Introduction

In this paper, we consider the efficient numerical schemes for solving the nonlocal water wave model

$$u_t + f(u)_x - \alpha u_{txx} + \mathcal{D}_x^\mu u = \nu u_{xx}, \tag{1}$$

where $u = u(x, t)$ represents the vertical displacement of the surface of the wave from its equilibrium, x is proportional to distance in the direction of wave and t is proportional to elapsed time. $\mathcal{D}_x^\mu$ is the linear combination of left and right Riemann–Liouville fractional derivatives

$$\mathcal{D}_x^\mu u(x, t) = \left(\kappa_1 \, {}_aD_x^\mu + \kappa_2 \, {}_xD_b^\mu\right) u(x, t), \quad 0 < \mu < 1, \tag{2}$$

with ${}_aD_x^\mu$ and ${}_xD_b^\mu$ being left and right Riemann–Liouville fractional derivatives of order μ, respectively, defined by [1]

$${}_aD_x^\mu u(x, t) = \frac{1}{\Gamma(1-\mu)} \frac{\partial}{\partial x} \int_a^x (x-s)^{-\mu} u(s, t) ds, \tag{3}$$

and

$${}_xD_b^\mu u(x, t) = \frac{-1}{\Gamma(1-\mu)} \frac{\partial}{\partial x} \int_x^b (s-x)^{-\mu} u(s, t) ds. \tag{4}$$

* Corresponding author at: Department of Applied Mathematics, School of Sciences, Xi'an University of Technology, Xi'an, Shaanxi 710054, PR China.
E-mail addresses: mathlican@xaut.edu.cn (C. Li), szhao@bama.ua.edu (S. Zhao).

http://dx.doi.org/10.1016/j.camwa.2015.11.018
0898-1221/

Here the parameters α, ν and κ_1, κ_2 are nonnegative constants which describe the balance, the effects of viscosity and dispersion. And the Fourier symbol of the operator of the fractional derivative defined in (2) gives [2,3]

$$\mathcal{F}(\mathcal{D}_x^{\mu}) = \kappa_1(ik)^{\mu} + \kappa_2(-ik)^{\mu} = \left[\cos\left(\frac{\pi\mu}{2}\right) + i(\kappa_1 - \kappa_2)\sin\left(\frac{\pi\mu}{2}\right)\right]|k|^{\mu}, \quad k \in \mathbb{R},\ i^2 = -1. \tag{5}$$

Equations of the form (1) appear in many models concerning the propagation of small-amplitude, nonlinear, dispersive, dissipative wave equations, see [4,5] and references therein. The evolution Eq. (1) includes several classical equations as special cases. For example, if $f(u) = u + \delta\frac{u^2}{2}$, $\delta > 0$, $\nu = 0$, $\mu = \frac{1}{2}$, the model reduces to fractional Kakutani–Matsuuchi model [5,6]

$$u_t + u_x - \alpha u_{txx} + \mathcal{D}_x^{\frac{1}{2}} u + \delta u u_x = 0. \tag{6}$$

If $\alpha = 0, f(u) = \frac{u^2}{2}$, the model reduces to the fractional Fowler equation [7,8]

$$u_t + u u_x + \mathcal{D}_x^{\mu} u = \nu u_{xx}. \tag{7}$$

And if $\nu = 0, f(u) = 0, \mu = \frac{1}{2}$, the model reduces to the fractional water wave equation [9]

$$u_t + \mathcal{D}_x^{\frac{1}{2}} u = 0. \tag{8}$$

The above mentioned models are Boussinesq systems with a nonlocal viscous term, they play more and more important role in investing the effect of viscosity on the gravity wave. In the previous studies, theoretical analysis for the nonlinear differential equations with a nonlocal term has been investigated [10–14]. For the well-posedness, regularity and asymptotic behaviors of solutions of the Cauchy problem for (6) with fractional Laplace operator (5), one can see [4,5]. Many different numerical methods, including some high order and fast algorithms [15–26], have been developed in the literature for the computation of linear fractional differential equations. In contrast to the linear problem, there are not many works on numerical methods for the nonlinear partial differential equations involving the fractional derivatives. A brief overview of the numerical studies for nonlinear fractional differential equations are given below. Biler et al. [27] developed a numerical method based on the interacting particles approximation for the solution of a large class of evolution problems involving the fractional Laplacian and a non-local quadratic-type non-linearity. Ervin et al. [28] developed a fully finite element approximation to a time dependent fractional diffusion equation which contains a nonlocal quadratic nonlinearity. Recently, Droniou [10] constructed a class of finite difference schemes with one order for the fractal conservation laws. It is proved that the numerical solutions converge toward Alibaud's entropy solution. The discontinuous Galerkin approximation of nonlinear conservation law with fractional Laplace operator has been discussed and a Kuznetsov type of theory has been established and applied to obtain the error estimates, see [29]. A Runge–Kutta local discontinuous Galerkin method has been proposed and stability and error estimations were derived for nonlinear conservation law with fractional Laplace operator in [30] by Xu and Hesthaven. In Chen's recent work [5], a Fourier spectral approximation was used to capture the time decay behavior of Eq. (6). Jennings discussed some efficient numerical methods for the fractional water wave equation (8) in unbounded domains with nonreflecting boundaries [9]. More recently, a semi-implicit spectral defect correction method is constructed for a nonlocal Kakutani–Matsuuchi model [31].

The main purpose of this work is to develop and investigate some effective difference techniques for fractional water waves model (1) on a finite domain. With the help of the weighted and shifted Grünwald–Letnikov (WSGL) formula, which was originally developed in Ref. [18] to approximate the nonlocal fractional operators, we design a series of second order accurate difference schemes for the model (1) with the linear and nonlinear convection terms. Moreover, we prove the existence and the uniqueness of the solution for the proposed schemes and study the properties of the numerical solutions. We show that our schemes are unconditionally convergent with second-order accuracy in both temporal and space accuracy. To our best acknowledge, stable and second order accurate difference methods have never been constructed before in the literature for solving the model equation (1).

The rest of the paper is organized as follows. In Section 2, we introduce some notations and then briefly review the second difference discretizations of fractional derivatives. In Section 3, we first design numerical scheme for model (1) with linear convection, i.e., $f(u) = u$. Later, we discuss the associated stability estimates and convergence analysis of the presented difference schemes. Then, we discretize the nonlinear equation (1) with nonlinear convection $f(u) = u^2/2$. We discretize the model (1) in time via a second-order Crank–Nicolson-differentiation formula. The nonlinear term in Eq. (1) is treated by linearization in our algorithm so that the linear iteration is solved at each time-step. The existence, stability and error estimates of our presented numerical schemes are established. We demonstrate the desired performance of the proposed numerical schemes in Section 5 by extensive numerical examples. The numerical results reported in this section are in good agreement with the theoretical estimates and thus demonstrate the effectiveness of the proposed method. And we examine the effect of different parameters appearing in model (1). The numerical simulations show that the value of μ has significant effect on the profiles of the solutions of the presented models. Finally, we give our conclusion in Section 6.

2. Weighted and shifted Grünwald–Letnikov (WSGL) operator

We start by introducing the necessary notations. Let $\{t_n\}_{n=0}^N$ be an equidistant partition of $[0, T]$ such that $t_n = n\tau$, where $\tau = \frac{T}{N}$ and $\{x_j\}_{j=0}^J$ be a partition of (a, b) such that $x_j = a + jh$, where $h = \frac{b-a}{J}$. Denote the function space $V_h = \left\{v = (v_j),\ v_0 = v_j = 0;\ 0 \le j \le J\right\}$. Let u_j^n be the numerical approximation of $u(x_j, t_n)$ i.e., $u_j^n \approx u(x_j, t_n)$, we introduce the following notations:

$$D_t u_j^n = \frac{u_j^{n+1} - u_j^n}{\tau}, \qquad D_+ u_j^n = \frac{u_{j+1}^n - u_j^n}{h}, \qquad D_- u_j^n = \frac{u_j^n - u_{j-1}^n}{h},$$
$$D_0 u_j^n = \frac{u_{j+1}^n - u_{j-1}^n}{2h}, \qquad D^2 u_j^n = D_+ D_- u_j^n = \frac{u_{j+1}^n - 2u_j^n + u_{j-1}^n}{h^2},$$
$$(u^n, v^n)_h = \sum_{j=0}^{J-1} h u_j^n v_j^n, \qquad \|u^n\|_h = \sqrt{(u^n, u^n)}, \qquad \|u^n\|_{\infty,h} = \max_{0\le j\le J-1} |u_j^n|, \tag{9}$$

$$|u^n|_{1,h}^2 = \sum_{j=0}^{J-1} h(D_+ u_j^n)^2, \qquad \|u^n\|_{1,h}^2 = \|u^n\|_h^2 + |u^n|_{1,h}^2 \tag{10}$$

and we can easily check that [32]

$$\sum_{j=0}^{J-1} \left[u_j^n D_0 \left(u_j^{n+\frac{1}{2}} \right) + D_0 \left(u_j^n u_j^{n+\frac{1}{2}} \right) \right] u_j^{n+\frac{1}{2}} = 0, \quad \text{with } u_0^n = 0,\ u_J^n = 0, \tag{11}$$

where $u_j^{n+\frac{1}{2}} = (u_j^n + u_j^{n+1})/2$.

Different definitions of fractional derivatives, such as the Grünwald–Letnikov derivative, Riemann–Liouville derivative, the Caputo derivative, and other modified definitions are introduced in the practical application [1]. And the Grünwald–Letnikov derivatives is more suitable for numerical approximation. It is usually used to approach the Riemann–Liouville derivative. For a function $u(x) \in C[a, b]$ with $u(a) = 0$, the relation between left Grünwald–Letnikov and left Riemann–Liouville derivative gives [1]

$${}_aD_x^\mu u(x) = \frac{1}{h^\mu} \sum_{k=0}^{\left[\frac{x-a}{h}\right]} w_k^{(\mu)} u(x - kh) + O(h). \tag{12}$$

And, for a function $u(x) \in C[a, b]$ with $u(b) = 0$, the relation between right Grünwald–Letnikov and right Riemann–Liouville derivative gives

$${}_xD_b^\mu u(x, t) = \frac{1}{h^\mu} \sum_{k=0}^{\left[\frac{b-x}{h}\right]} w_k^{(\mu)} u(x + kh) + O(h) \tag{13}$$

where $\Gamma(\cdot)$ is the Gamma function, and $w_k^{(\mu)} := \frac{\Gamma(k-\mu)}{\Gamma(-\mu)\Gamma(k+1)} = (-1)^k \binom{\mu}{k}$ is the normalized Grünwald weights. However, the difference scheme based on the Grünwald–Letnikov formula for time dependent problems is unstable [15]. To overcome this problem, Meerschaert and Tadjeran in [15,16] firstly introduced the shifted Grünwald–Letnikov approximation formula

$${}_aD_x^\mu u(x) = \frac{1}{h^\mu} \sum_{k=0}^{\left[\frac{x-a}{h}\right]+p} w_k^{(\mu)} u(x - (k-p)h) + O(h), \tag{14}$$

$${}_xD_b^\mu u(x) = \frac{1}{h^\mu} \sum_{k=0}^{\left[\frac{b-x}{h}\right]+p} w_k^{(\mu)} u(x + (k-p)h) + O(h). \tag{15}$$

To improve the truncation error in above relations (14) and (15), Tian et al. [18] introduced the second order weighted and shifted Grünwald–Letnikov (WSGD) operators for the left and right Riemann–Liouville derivatives. If function $u(x) \in C^3[a, b]$, the three parameters WSGD operators in finite domain $[a, b]$ can be written as the following form [33]

$$\begin{aligned}
{}_L\mathcal{D}_{h,1,0,-1}^{\mu,\lambda_1,\lambda_2,\lambda_3} u(x) &= \frac{\lambda_1}{h^\mu} \sum_{k=0}^{\left[\frac{x-a}{h}\right]+1} w_k^{(\mu)} u(x - (k-1)h) + \frac{\lambda_2}{h^\mu} \sum_{k=0}^{\left[\frac{x-a}{h}\right]} w_k^{(\mu)} u(x - kh) + \frac{\lambda_3}{h^\mu} \sum_{k=0}^{\left[\frac{x-a}{h}\right]-1} w_k^{(\mu)} u(x - (k+1)h), \\
{}_R\mathcal{D}_{h,1,0,-1}^{\mu,\lambda_1,\lambda_2,\lambda_3} u(x) &= \frac{\lambda_1}{h^\mu} \sum_{k=0}^{\left[\frac{b-x}{h}\right]+1} w_k^{(\mu)} u(x + (k-1)h) + \frac{\lambda_2}{h^\mu} \sum_{k=0}^{\left[\frac{b-x}{h}\right]} w_k^{(\mu)} u(x + kh) + \frac{\lambda_3}{h^\mu} \sum_{k=0}^{\left[\frac{b-x}{h}\right]-1} w_k^{(\mu)} u(x + (k+1)h),
\end{aligned} \tag{16}$$

where the parameters $\lambda_j,\ j = 1, 2, 3$, satisfying the following linear system

$$\begin{cases} \lambda_1 + \lambda_2 + \lambda_3 = 1, \\ \lambda_1 - \lambda_3 = \dfrac{\mu}{2}. \end{cases} \tag{17}$$

The solutions of the linear system (17) can be collected by the following three sets

$$\mathcal{S}_1^{\mu} = \left\{ \lambda_1 \text{ is given},\ \lambda_2 = \frac{2+\mu}{2} - 2\lambda_1,\ \lambda_3 = \lambda_1 - \frac{\mu}{2} \right\} \tag{18}$$

or

$$\mathcal{S}_2^{\mu} = \left\{ \lambda_1 = \frac{2+\mu}{4} - \frac{\lambda_2}{2},\ \lambda_2 \text{ is given},\ \lambda_3 = \frac{2-\mu}{4} - \frac{\lambda_2}{2} \right\} \tag{19}$$

or

$$\mathcal{S}_3^{\mu} = \left\{ \lambda_1 = \frac{\mu}{2} + \lambda_3,\ \lambda_2 = \frac{2-\mu}{2} - 2\lambda_3,\ \lambda_3 \text{ is given} \right\}. \tag{20}$$

For any choice of scalar $\lambda_j,\ j = 1, 2, 3$, the set $\mathcal{S}_j^{\mu},\ j = 1, 2, 3$ is the solution to linear system (17). It produces a second-order approximation if we take any choice of $\lambda_j,\ j = 1, 2, 3$ in $\mathcal{S}_j^{\mu},\ j = 1, 2, 3$. Particularly, if we take $\lambda_j = 0$ for $j = 1, 2, 3$ in $\mathcal{S}_j^{\mu},\ j = 1, 2, 3$, it recovers the second-order approximations presented in [18]. After rearranging the weights $w_k^{(\mu)}$ in (16), the Riemann–Liouville fractional derivatives of function $u(x)$ at point x_j can be approximated as

$$\begin{aligned} {}_aD_x^{\mu} u(x_j) &= \frac{1}{h^{\mu}} \sum_{k=0}^{j+1} g_k^{(\mu)} u(x_{j-k+1}) + O(h^2), \\ {}_xD_b^{\mu} u(x_j) &= \frac{1}{h^{\mu}} \sum_{k=0}^{J-j+1} g_k^{(\mu)} u(x_{j+k-1}) + O(h^2), \end{aligned} \tag{21}$$

where the weights are given as

$$\begin{aligned} &g_0^{(\mu)} = \lambda_1 w_0^{(\mu)}, \qquad g_1^{(\mu)} = \lambda_1 w_1^{(\mu)} + \lambda_2 w_0^{(\mu)}, \\ &g_k^{(\mu)} = \lambda_1 w_k^{(\mu)} + \lambda_2 w_{k-1}^{(\mu)} + \lambda_3 w_{k-2}^{(\mu)}, \quad k \geq 2. \end{aligned} \tag{22}$$

Note that if the parameters $\lambda_j,\ j = 1, 2, 3$, in (21) are taken as

$$\lambda_1 = \frac{3\mu^2 + 5\mu}{24}, \qquad \lambda_2 = \frac{12 - 3\mu^2 + \mu}{12}, \qquad \lambda_3 = \frac{3\mu^2 - 7\mu}{24}, \tag{23}$$

then the corresponding WSGD operators have third order accuracy. However, for the fractional PDEs with time evolution, the numerical scheme with third order WSGD operator maybe be unstable. Hence, we pay our attention on the second order WSGD operators in the following sections.

3. Difference schemes for linear water wave model

We first consider the initial–boundary value problem of the linear fractional Fowler equation [8]

$$\begin{cases} u_t + u_x + \mathcal{D}_x^{\mu} u = \nu u_{xx} + s(x,t), & (x,t) \in (a,b) \times [0,T], \\ u(x,0) = u_0(x), & x \in (a,b), \\ u(a,t) = \varphi_a(t), \qquad u(b,t) = \varphi_b(t), & t \in [0,T], \end{cases} \tag{24}$$

where $s(x,t)$ is the source term, ν is diffusion coefficient, and $\mathcal{D}_x^{\mu}$ is defined by formula (2). The diffusion coefficients κ_1 and κ_2 are nonnegative constants with $\kappa_1^2 + \kappa_2^2 \neq 0$. The Dirichlet boundary data is assumed to be dependent on the diffusion coefficients. In particular, if $\kappa_1 \neq 0$, then $\phi_a(t) \equiv 0$; if $\kappa_2 \neq 0$, then $\phi_b(t) \equiv 0$. In the analysis of the numerical method, we assume that (24) has a unique and sufficiently smooth solution.

In space discretization, we choose the WSGD operators ${}_L\mathcal{D}_{h,1,0,-1}^{\mu,\lambda_1,\lambda_2,\lambda_3} u(\cdot,t)$ and ${}_R\mathcal{D}_{h,1,0,-1}^{\mu,\lambda_1,\lambda_2,\lambda_3} u(\cdot,t)$ defined in (16) to approximate the Riemann–Liouville fractional derivatives ${}_aD_x^{\mu} u(\cdot,t)$ and ${}_xD_b^{\mu} u(\cdot,t)$, respectively. And the first order space derivative is approximated by the standard central difference. If the time derivative is approximated by the Crank–Nicolson time discretization, we have

$$D_t u_j^n + D_0 \left(u_j^{n+\frac{1}{2}} \right) + \left(\kappa_1 \, {}_L\mathcal{D}_{h,1,0,-1}^{\mu,\lambda_1,\lambda_2,\lambda_3} + \kappa_2 \, {}_R\mathcal{D}_{h,1,0,-1}^{\mu,\lambda_1,\lambda_2,\lambda_3} \right) u_j^{n+\frac{1}{2}} = \nu D^2 \left(u_j^{n+\frac{1}{2}} \right) + s_j^{n+\frac{1}{2}} + O(\tau^2 + h^2).$$

Dropping truncation error term, we propose the following Crank–Nicolson-WSGD scheme

$$D_t u_j^n + D_0\left(u_j^{n+\frac{1}{2}}\right) + \left(\kappa_1\, {}_L\mathcal{D}_{h,1,0,-1}^{\mu,\lambda_1,\lambda_2,\lambda_3} + \kappa_2\, {}_R\mathcal{D}_{h,1,0,-1}^{\mu,\lambda_1,\lambda_2,\lambda_3}\right)u_j^{n+\frac{1}{2}} = \nu D^2\left(u_j^{n+\frac{1}{2}}\right) + s_j^{n+\frac{1}{2}}. \tag{25}$$

If denote $U^n = \left(u_1^n, u_2^n, \ldots, u_{J-1}^n\right)^{\mathrm{T}}$, then the above numerical scheme can be rewritten as the following form

$$\left(I + \frac{\tau}{4h}B + \frac{\tau}{2h^\mu}(\kappa_1 A_\mu + \kappa_2 A_\mu^{\mathrm{T}}) - \frac{\nu\tau}{h^2}C\right)U^{n+1} = \left(I - \frac{\tau}{4h}B - \frac{\tau}{2h^\mu}(\kappa_1 A_\mu + \kappa_2 A_\mu^{\mathrm{T}}) + \frac{\nu\tau}{h^2}C\right)U^n + \tau S^{n+\frac{1}{2}}, \tag{26}$$

where $B = tridiag\{-1, 0, 1\}$ is also an anti-symmetric tri-diagonal matrix of $J-1$-square, $C = tridiag\{1, -2, 1\}$ is a symmetric tri-diagonal matrix of $J-1$-square, and A_μ is given by

$$A_\mu = \begin{pmatrix} g_1^{(\mu)} & g_0^{(\mu)} & & & \\ g_2^{(\mu)} & g_1^{(\mu)} & g_0^{(\mu)} & & \\ \vdots & g_2^{(\mu)} & g_1^{(\mu)} & \ddots & \\ g_{J-2}^{(\mu)} & \cdots & \ddots & \ddots & g_0^{(\mu)} \\ g_{J-1}^{(\mu)} & g_{J-2}^{(\mu)} & \cdots & g_2^{(\mu)} & g_1^{(\mu)} \end{pmatrix}_{J-1\times J-1}, \tag{27}$$

and

$$\begin{aligned} S^{n+\frac{1}{2}} = {} & \begin{pmatrix} s_1^{n+\frac{1}{2}} \\ s_2^{n+\frac{1}{2}} \\ \vdots \\ s_{J-2}^{n+\frac{1}{2}} \\ s_{J-1}^{n+\frac{1}{2}} \end{pmatrix} + \frac{1}{2h^\mu}\begin{pmatrix} \kappa_1 g_2^{(\mu)} + \kappa_2 w_0^{(\mu)} \\ \kappa_1 g_3^{(\mu)} \\ \vdots \\ \kappa_1 g_{J-1}^{(\mu)} \\ \kappa_1 g_J^{(\mu)} \end{pmatrix} u_0^{n+\frac{1}{2}} + \frac{1}{4h}\begin{pmatrix} u_0^n + u_0^{n+1} \\ 0 \\ \vdots \\ 0 \\ u_J^n + u_J^{n+1} \end{pmatrix} \\ & + \frac{\nu}{2h^2}\begin{pmatrix} u_0^{n+\frac{1}{2}} \\ 0 \\ \vdots \\ 0 \\ u_J^{n+\frac{1}{2}} \end{pmatrix} + \frac{1}{2h^\mu}\begin{pmatrix} \kappa_2 g_J^{(\mu)} \\ \kappa_2 g_{J-1}^{(\mu)} \\ \vdots \\ \kappa_2 g_3^{(\mu)} \\ \kappa_1 g_0^{(\mu)} + \kappa_2 w_2^{(\mu)} \end{pmatrix} u_J^{n+\frac{1}{2}}. \end{aligned} \tag{28}$$

Here u_0^n and u_0^J are given by the boundary values $\varphi_a(t)$ and $\varphi_b(t)$ at t_n, respectively.

3.1. Stability and convergence analysis

Next, we carry out the stability and convergence of the difference scheme (25). Our analysis is based on the ideas developed in [18,33]. To establish the error estimate we will use the following lemmas.

Lemma 1 ([34]). *A matrix $A \in \mathbb{R}^{n\times n}$ is positive definite if and only if its symmetric part $H = \frac{A+A^T}{2}$ is positive definite; H is positive definite if and only if the eigenvalues of H are positive.*

Lemma 2 ([34]). *If $A \in \mathbb{C}^{n\times n}$, let $H = \frac{A+A^*}{2}$ be the hermitian part of A, A^* the conjugate transpose of A, then for any eigenvalue μ of A, there exists*

$$\gamma_{\min}(H) \le \mathrm{Re}(\mu(\mathrm{H})) \le \gamma_{\max}(H),$$

where $\mathrm{Re}(\mu(\mathrm{H}))$ *represents the real part of* $\mu(H)$, *and* $\mu_{\min}(H)$ *and* $\mu_{\max}(H)$ *are the minimum and maximum of the eigenvalues of* H.

Definition 1 ([35]). Let the Toeplitz matrix T_n be of the following form,

$$T_n = \begin{pmatrix} t_0 & t_{-1} & \cdots & t_{2-n} & t_{1-n} \\ t_1 & t_0 & t_{-1} & \cdots & t_{2-n} \\ \vdots & t_1 & t_0 & \ddots & \vdots \\ t_{n-2} & \cdots & \ddots & \ddots & t_{-1} \\ t_{n-1} & t_{n-2} & \cdots & t_1 & t_0 \end{pmatrix};$$

if the diagonals $\{t_k\}_{k=-n+1}^{n-1}$ are the Fourier coefficients of a function f, i.e.,

$$t_k = \frac{1}{2\pi}\int_{-\pi}^{\pi} f(x)\mathrm{e}^{-ikx}dx,$$

then the function f is called the generating function of T_n.

Lemma 3 (*Grenander–Szegö Theorem [35]*). *For the above Toeplitz matrix T_n, denote $\mu_{\min}(T_n)$ and $\mu_{\max}(T_n)$ as the smallest and largest eigenvalues of T_n, respectively; if f is a 2π-periodic continuous real-valued function defined on $[-\pi, \pi]$, then we have*

$$f_{\min} \le \gamma_{\min}(T_n) \le \gamma_{\max}(T_n) \le f_{\max},$$

where $f_{\min}$ and $f_{\max}$ denote the minimum and maximum values of $f(x)$. Moreover, if $f_{\min} < f_{\max}$, then all the eigenvalues of T_n satisfy

$$f_{\min} < \gamma(T_n) < f_{\max},$$

for all $n > 0$; and furthermore if $f_{\min} \ge 0$, then T_n is positive definite.

Lemma 4 (*[36]*). *If $P \in \mathbb{C}^{n\times n}$ and $P + Q \in \mathbb{C}^{n\times n}$ are symmetric matrices, then*

$$\gamma_k(P) + \gamma_m(Q) \le \gamma_k(P+Q) \le \gamma_k(P) + \gamma_1(Q), \quad k = 1, 2, \ldots, m;\ m \le n,$$

with eigenvalues $\gamma_1(\cdot) \ge \gamma_2(\cdot) \ge \cdots \ge \gamma_m(\cdot)$.

Lemma 5. *Let the weighted parameters $(\lambda_1, \lambda_2, \lambda_3)$ be chosen in set $\mathcal{S}_1^{\mu}(\lambda_1, \lambda_2, \lambda_3)$ or $\mathcal{S}_2^{\mu}(\lambda_1, \lambda_2, \lambda_3)$ or $\mathcal{S}_3^{\mu}(\lambda_1, \lambda_2, \lambda_3)$, and assume that the real part of trigonometric polynomial $Q(\mu, x; \lambda_1, \lambda_2, \lambda_3)$ defined by (31) is non-negative, i.e. $Q(\mu, x; \lambda_1, \lambda_2, \lambda_3) \ge 0$, for all $x \in [-\pi, \pi]$, $0 < \mu < 1$. For the weight coefficients $g_k^{(\mu)}$ given in (22), for any positive integer k and real vector $v = (v_1, v_2, \ldots, v_{J-1})^T \in R^{J-1}$, it holds that*

$$\sum_{j=1}^{J-1}\Big(\sum_{k=0}^{j+1} g_k^{(\mu)} v_{j+1-k}\Big)v_j \ge 0,$$

and

$$\sum_{j=1}^{J-1}\Big(\sum_{k=0}^{J-j+1} g_k^{(\mu)} v_{j-1+k}\Big)v_j \ge 0.$$

Proof. One can easily check that

$$\sum_{j=1}^{J-1}\Big(\sum_{k=0}^{j+1} g_k^{(\mu)} v_{j+1-k}\Big)v_j = \big(A_\mu v, v\big), \tag{29}$$

and

$$\sum_{j=1}^{J-1}\Big(\sum_{k=0}^{J-j+1} g_k^{(\mu)} v_{j-1+k}\Big)v_j = \big(A_\mu^T v, v\big), \tag{30}$$

where the matrix A_μ is given in (27). Hence to prove that the above quadratic form is non-negative is equivalent to prove that the symmetric Toeplitz matrix $H = \frac{A_\mu + A_\mu^T}{2}$ is positive semi-definite. By simple calculation, we get the generating function of H gives

$$Q(\mu, x; \lambda_1, \lambda_2, \lambda_3) = \left(\frac{\lambda_1}{2}\cos\Big(\frac{\mu}{2}(x-\pi) - x\Big) + \frac{\lambda_2}{2}\cos\Big(\frac{\mu}{2}(x-\pi)\Big) + \frac{\lambda_3}{2}\cos\Big(\frac{\mu}{2}(x-\pi) + x\Big)\right). \tag{31}$$

With the similar method used in [18], we can only check that the generating function of H is non-negative. For more details, see [18]. □

Remark 1. Since $Q(\mu, x; \lambda_1, \lambda_2, \lambda_3)$ is a real-valued and even function about variable x, we just consider its principal value on $[0, \pi]$. And there do exist real parameters $(\lambda_1, \lambda_2, \lambda_3)$ in $\mathcal{S}_1^{\mu}$ or $\mathcal{S}_2^{\mu}$ or $\mathcal{S}_3^{\mu}$ such that $Q(\mu, x; \lambda_1, \lambda_2, \lambda_3) \ge 0$ holds for all $x \in [0, \pi]$, $0 < \mu < 1$. For example, for $(\lambda_1, \lambda_2, \lambda_3) = (0, \frac{2+\mu}{2}, -\frac{\mu}{2})$, we have

$$Q\left(\mu, x; 0, \frac{2+\mu}{2}, -\frac{\mu}{2}\right) = \left(2\sin\left(\frac{x}{2}\right)\right)^{\mu}\left(\frac{2+\mu}{2}\cos\Big(\frac{\mu}{2}(x-\pi)\Big) - \frac{\mu}{2}\cos\Big(\frac{\mu}{2}(x-\pi) + x\Big)\right). \tag{32}$$

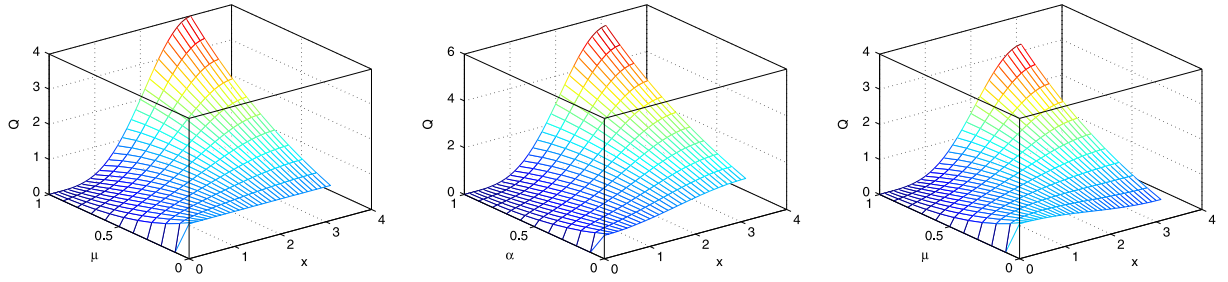

(a) $\lambda_1 = 0$. (b) $\lambda_1 = -0.2$. (c) $\lambda_1 = 0.1$.

Fig. 1. The trigonometric polynomials $Q(\mu, x; \lambda_1, \lambda_2, \lambda_3)$, where the parameters $(\lambda_1, \lambda_2, \lambda_3)$ are selected in set $\mathcal{S}_1^\mu$.

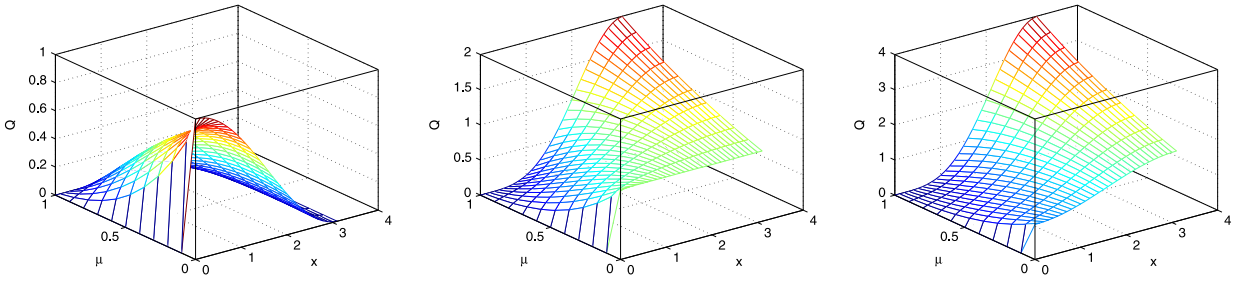

(a) $\lambda_2 = 0.5$. (b) $\lambda_2 = 1$. (c) $\lambda_2 = 1.5$.

Fig. 2. The trigonometric polynomials $Q(\mu, x; \lambda_1, \lambda_2, \lambda_3)$, where the parameters $(\lambda_1, \lambda_2, \lambda_3)$ are selected in set $\mathcal{S}_2^\mu$.

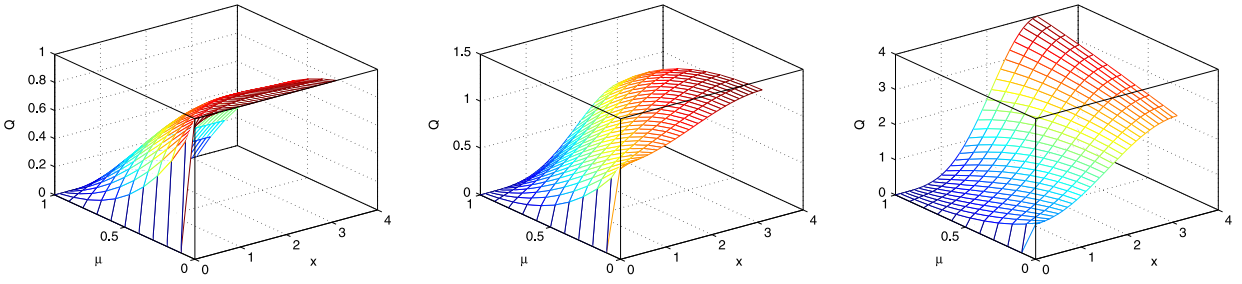

(a) $\lambda_3 = 0$. (b) $\lambda_3 = -0.1$. (c) $\lambda_3 = -0.5$.

Fig. 3. The trigonometric polynomials $Q(\mu, x; \lambda_1, \lambda_2, \lambda_3)$, where the parameters $(\lambda_1, \lambda_2, \lambda_3)$ are selected in set $\mathcal{S}_3^\mu$.

It is easy to check that $Q(\mu, x; 0, \frac{2+\mu}{2}, -\frac{\mu}{2})$ is nondecreasing with respect to x, then [21]

$$Q\left(\mu, x; 0, \frac{2+\mu}{2}, -\frac{\mu}{2}\right) \geq Q\left(\mu, 0; 0, \frac{2+\mu}{2}, -\frac{\mu}{2}\right) \geq 0.$$

However, it seems not easy to analytically generate the effective regions for the parameters $(\lambda_1, \lambda_2, \lambda_3)$ from $Q(\mu, x; \lambda_1, \lambda_2, \lambda_3)$. Fortunately, this can be easily done through the numerical test, see the following numerical experiment section. After selecting the weight parameters λ_j, $j = 1, 2, 3$, the practical stability criterion $Q(\mu, x; \lambda_1, \lambda_2, \lambda_3) \geq 0$ can be numerically checked easily. In Figs. 1–3, we plot the trigonometric polynomials $Q(\mu, x; \lambda_1, \lambda_2, \lambda_3)$. With the chosen parameters, it can further be seen that the hypothesis presented in Lemma 5 is satisfied.

Then it follows from Lemma 5, we have

Corollary 1. *Let $(\lambda_1, \lambda_2, \lambda_3)$ be chosen in set $\mathcal{S}_1^\mu$ or $\mathcal{S}_2^\mu$ or $\mathcal{S}_3^\mu$, and assume that the trigonometric polynomial satisfies $Q(\mu, x; \lambda_1, \lambda_2, \lambda_3) \geq 0$, for all $x \in [-\pi, \pi]$, $0 < \mu < 1$, and matrix A_μ be defined by (27), then the real parts of eigenvalues of A_μ are non-negative. Moreover, for all $\kappa_1, \kappa_2 \geq 0$, $\kappa_1^2 + \kappa_2^2 \neq 0$, the real parts of eigenvalues of $\kappa_1 A_\mu + \kappa_2 A_\mu^T$ are also non-negative.*

Theorem 1. *Let $(\lambda_1, \lambda_2, \lambda_3)$ be chosen in set $\mathcal{S}_1^\mu$ or $\mathcal{S}_2^\mu$ or $\mathcal{S}_3^\mu$, and assume that the trigonometric polynomial satisfies $Q(\mu, x; \lambda_1, \lambda_2, \lambda_3) \geq 0$, for all $x \in [-\pi, \pi]$, $0 < \mu < 1$, then the Crank–Nicolson-WSGD scheme (25) is unconditionally stable, where $Q(\mu, x; \lambda_1, \lambda_2, \lambda_3)$ is defined by (31).*

Proof. Let $\widetilde{u}_j^n$ be the another approximate solution. Putting $\epsilon_j^n = \widetilde{u}_j^n - u_j^n$, and denoting $E^n = (\epsilon_1^n, \epsilon_2^n, \ldots, \epsilon_{J-1}^n)^T$, then from (25) and (24) we obtain the following perturbation equation

$$(I - D)E^{n+1} = (I + D)E^n,$$

where

$$D = -\frac{\tau}{4h}B - \frac{\tau}{h^\mu}(\kappa_1 A_\mu + \kappa_2 A_\mu^{\mathrm{T}}) + \frac{\nu\tau}{h^2}C. \tag{33}$$

From (33), there exists

$$\frac{D + D^T}{2} = H_1 + H_2, \quad H_1 = -\frac{\tau(\kappa_1 + \kappa_2)}{h^\mu}\frac{A_\mu + A_\mu^T}{2},\ H_2 = \frac{\nu\tau}{h^2}\frac{C + C^T}{2}.$$

Denote $\gamma(D)$ be an eigenvalue of the matrix D, then the eigenvalue of the matrix $(I-D)^{-1}(I+D)$ gives $(1-\gamma(D))^{-1}(1+\gamma(D))$. Moreover, due to the matrices H_1 and H_2 are both negative definite and symmetric matrices, it follows that $\gamma_k(H_1 + H_2)$ are real valued and symmetric matrices, according to Lemma 4, we get

$$\gamma_k(H_1 + H_2) < \gamma_k(H_1) + \gamma_1(H_2) < 0.$$

Furthermore, using Lemma 4, we get $\mathrm{Re}(\gamma(D)) < 0$. Hence, it implies that $|(1-\gamma(D))^{-1}(1+\gamma(D))| < 1$. Thus, the spectral radius of the matrix $(I - D)^{-1}(I + D)$ is less than 1. Finally, we conclude that the numerical scheme (25) is unconditionally stable. □

Theorem 2. *Let $(\lambda_1, \lambda_2, \lambda_3)$ be chosen in set $\mathcal{S}_1^\mu$ or $\mathcal{S}_2^\mu$ or $\mathcal{S}_3^\mu$ such that the trigonometric polynomial $Q(\mu, x; \lambda_1, \lambda_2, \lambda_3) \geq 0$, for all $x \in [-\pi, \pi]$, $0 < \mu < 1$, let $u(x_j, t_n)$ be the exact solution of (24) with $1 < \mu < 1$, and u_j^n be solution of Crank–Nicolson-WSGD scheme (25), then we have*

$$\|u(x_j, t_n) - u_j^n\|_h \leq C(\tau^2 + h^2), \quad j = 1, 2, \ldots, J-1;\ n = 0, 1, \ldots, N,$$

where $Q(\mu, x; \lambda_1, \lambda_2, \lambda_3)$ is defined by (31).

Proof. Denoting $e_j^n = u(x_j, t_n) - u_j^n$, and $e^n = [e_1^n, e_2^n, \ldots, e_{J-1}^n]^T$. Subtracting (24) from (25) and using $e^0 = 0$, we obtain

$$(I - D)e^{n+1} = (I + D)e^n + R^n,$$

where D is defined by (33), and $R^n = [R_1^n, R_2^n, \ldots, R_{J-1}^n]^T$. The above equation can be rewritten as

$$e^{n+1} = (I - D)^{-1}(I + D)e^n + (I - D)^{-1}R^n.$$

Taking the L^2-norm on both sides of above equation, we obtain

$$\|e^n\|_h \leq \|(I - D)^{-1}(I + D)e^{n-1}\|_h + \|(I - D)^{-1}R^n\|_h.$$

We further find that

$$\begin{aligned}\|e^n\|_h &\leq \|(I - D)^{-1}(I + D)e^{n-1}\|_h + \|(I - D)^{-1}R^n\|_h \\ &\leq \|(I - D)^{-1}(I + D)\|_2\, \|e^{n-1}\|_h + \|(I - D)^{-1}\|_2\, \|R^n\|_h\end{aligned}$$

where $\|\cdot\|_2$ denotes the 2-norm of a matrix. With the similar argument presented in [18], we can prove that

$$\|(I - D)^{-1}(I + D)\|_2 \leq 1, \qquad \|(I - D)^{-1}\|_2 \leq 1.$$

Since the truncation error gives $|R_j^n| \leq C\tau(\tau^2 + h^2)$, we obtain

$$\|e^n\|_h \leq \|e^{n-1}\|_h + \|R^n\|_h \leq \sum_{k=1}^{n} \|R^k\|_h \leq C(\tau^2 + h^2). \quad \square$$

4. Linearized difference schemes for nonlinear water wave model

Now we consider the initial–boundary value problem of fractional Kakutani–Matsuuchi equation [4,5]

$$\begin{cases} u_t + u_x - \alpha u_{txx} + \mathcal{D}_x^\mu u + \delta u u_x = \nu u_{xx}, & (x, t) \in (a, b) \times [0, T], \\ u(x, 0) = u_0(x), & x \in (a, b), \\ u(a, t) = \varphi_a(t), u(b, t) = \varphi_b(t), & t \in [0, T], \end{cases} \tag{34}$$

where α, δ and ν are the dispersion, advection and diffusion coefficients, and $\mathcal{D}_x^\mu$ is defined by formula (2). We assume that the restriction on the diffusion coefficients κ_1 and κ_2 in (2) is the same as given in model (24). And we always assume that (34)

has a unique and sufficiently smooth solution in constructing our numerical schemes. Moreover, we use the Crank–Nicolson difference formula to discretize the first order time derivative. Hence, we can propose a Crank–Nicolson-WSGD scheme for model (34)

$$D_t u_j^n - \alpha D_t D^2 u_j^n + D_0 u_j^{n+\frac{1}{2}} + \left(\kappa_1 {}_L\mathcal{D}_{h,1,0,-1}^{\mu,\lambda_1,\lambda_2,\lambda_3} + \kappa_{2R}\mathcal{D}_{h,1,0,-1}^{\mu,\lambda_1,\lambda_2,\lambda_3}\right)u_j^{n+\frac{1}{2}} + \mathcal{N}(u_j^n) = \nu D^2 u_j^{n+\frac{1}{2}}, \tag{35}$$

where

$$\mathcal{N}(u_j^n) = \frac{\delta}{3}\left(u_j^n D_0 u_j^{n+\frac{1}{2}} + D_0\left(u_j^n u_j^{n+\frac{1}{2}}\right)\right),$$

and the initial condition is discretized as $u_j^0 = u_0(x_j)$. In the above linear system, $u_0^n = \varphi_a(t_n)$, $u_J^n = \varphi_b(t_n)$ and there is no need to solve a nonlinear algebraic system since the nonlinear term can be obtained by the previous time step. Denote the local truncation of difference scheme (35) as

$$R_j^n = D_t v_j^n + D_0 v_j^n - \alpha D_t D^2 v_j^n + (\kappa_1 {}_L\mathcal{D}_{h,1,0,-1}^{\mu,\lambda_1,\lambda_2,\lambda_3} + \kappa_2 {}_R\mathcal{D}_{h,1,0,-1}^{\mu,\lambda_1,\lambda_2,\lambda_3})v_j^{n+\frac{1}{2}} + \mathcal{N}\left(v_j^{n+\frac{1}{2}}\right) - \nu D^2 v_j^{n+\frac{1}{2}}, \tag{36}$$

where $v_j^n = u(x_j, t_n)$, $0 \le j \le J$, $0 \le n \le N$. By means of Taylor expansion, if $u(x,t) \in C^{3,2}\big((a,b)\times(0,T]\big)$, we get $R_j^n = O(\tau^2 + h^2)$.

4.1. Existence, stability and convergence of numerical solutions

In this section, we show the existence, stability and convergence of the numerical solutions. Unlike the analysis in linear scheme (26), we will employ the following Brouwer fixed point theorem.

Lemma 6 (*Brouwer Fixed Point Theorem [37]*). *Let H be a finite dimensional Hilbert space with inner product $(\cdot,\cdot)_H$ and induced norm $\|\cdot\|_H$, and assume that $\Phi : H \to H$ be a continuous function. If $(\Phi(x), x)_H > 0$ for all $x \in H$ with $\|x\|_H = \beta > 0$, then there exists $x^* \in H$, with $\|x^*\| < \beta$ such that $\Phi(x^*) = 0$.*

Theorem 3. *Let the weighted parameters $(\lambda_1, \lambda_2, \lambda_3)$ be chosen in set $\mathcal{S}_1^\mu(\lambda_1,\lambda_2,\lambda_3)$ or $\mathcal{S}_2^\mu(\lambda_1,\lambda_2,\lambda_3)$ or $\mathcal{S}_3^\mu(\lambda_1,\lambda_2,\lambda_3)$, and assume that the trigonometric polynomial $Q(\mu, x; \lambda_1, \lambda_2, \lambda_3)$ defined by (31) is non-negative, i.e., $Q(\mu, x; \lambda_1, \lambda_2, \lambda_3) \ge 0$, for all $x \in [-\pi, \pi]$, $0 < \mu < 1$. Then, for a positive integer J, and given $u^0 \in \mathbb{R}^{J-1}$, the Crank–Nicolson WSGD scheme (35) has a solution $\{u^n\}_{n=0}^N$.*

Proof. We use the mathematical induction to prove the theorem. Assume that we have $u^1, u^2, \ldots, u^n$ for $n < N$, we show u^{n+1} in the equation of (35). To do this, we introduce a function: $\Phi : \mathbb{R}^{J-1} \to \mathbb{R}^{J-1}$ by

$$\Phi(v) := 2v - 2u^n - (2\alpha D^2 v - 2\alpha D^2 u^n) + \tau D_0 v + \tau\mathcal{N}(v) + \tau\mathcal{D}_{h,1,0,-1}^{\mu,\lambda_1,\lambda_2,\lambda_3} v - \nu\tau D^2 v, \tag{37}$$

where

$$\mathcal{D}_{h,1,0,-1}^{\mu,\lambda_1,\lambda_2,\lambda_3} v = \left(\kappa_1 {}_L\mathcal{D}_{h,1,0,-1}^{\mu,\lambda_1,\lambda_2,\lambda_3} + \kappa_{2R}\mathcal{D}_{h,1,0,-1}^{\mu,\lambda_1,\lambda_2,\lambda_3}\right)v,$$

and

$$\mathcal{N}(v) = \delta\frac{u_j^n D_0 v_j^{n+\frac{1}{2}} + D_0\left(v_j^n v_j^{n+\frac{1}{2}}\right)}{3}.$$

Taking the L^2 inner in Eq. (37), we get

$$\begin{aligned}(\Phi(v), v)_h :=\ & 2\|v\|_h^2 - 2(u^n, v)_h + 2\alpha\|D_+ v\|_h^2 - 2\alpha(D_+ u^n, D_+ v)_h + \tau(\mathcal{N}(v), v)_h \\ & + \tau\left(\mathcal{D}_{h,1,0,-1}^{\mu,\lambda_1,\lambda_2,\lambda_3} v, v\right)_h - \tau\nu(D_+ D^2 v, v)_h.\end{aligned} \tag{38}$$

Furthermore, using the fact that

$$\left(\mathcal{N}(v), v\right)_h = \frac{1}{3}\sum_{j=0}^{J-1}\left(v_j^n D_0(v_j) + D_0(v_j^n v_j)\right)v_j = 0, \tag{39}$$

we have

$$(\Phi(v), v)_h = 2\|v\|_h^2 - 2(u^n, v)_h + 2\alpha\|D_+ v\|_h^2 - 2\alpha(D_+ u^n, D_+ v)_h + \tau\left(\mathcal{D}_{h,1,0,-1}^{\mu,\lambda_1,\lambda_2,\lambda_3} v, v\right)_h - \tau\nu(D^2 v, v)_h. \tag{40}$$

Combining the fact

$$\left(\mathcal{D}^{\mu,\lambda_1,\lambda_2,\lambda_3}_{h,1,0,-1}v, v\right)_h = \sum_{j=0}^{J-1}\left[\left(\kappa_1\sum_{k=0}^{j+1}g_k^{(\mu)}v_{j+1-k} + \kappa_2\sum_{k=0}^{J-j+1}g_k^{(\mu)}v_{j-1+k}\right)\right]v_j \geq 0$$

and

$$-\tau(D^2v, v)_h = -\tau(D_+D_-v, v)_h = \tau(D_+u^n, D_+v)_h = \tau|v|^2_{1,h} \geq 0$$

we have

$$\begin{aligned}(\Phi(v), v)_h &\geq 2\|v\|_h^2 - 2\|v\|\,\|u^n\|_h + 2\alpha|v|^2_{1,h} - 2\alpha|v|_{1,h}|u^n|_{1,h} &(41)\\ &\geq 2\|v\|_h^2 - (\|v\|_h^2 + \|u^n\|_h^2) + 2\alpha|v|^2_{1,h} - \alpha(|v|^2_{1,h} + |u^n|^2_{1,h})\\ &\geq \|v\|_h^2 - \|u^n\|_h^2 + \alpha|v|^2_{1,h} - \alpha|u^n|^2_{1,h} &(42)\\ &\geq \|v\|_h^2 - \|u^n\|^2_{1,h}.\end{aligned}$$

We can see that $(\Phi(v), v)_h > 0$ for all $v \in V_h$ with $\|v\|_h = \|u^n\|^2_{1,h} + 1$, where $\|u^n\|^2_{1,h} = \|u^n\|_h^2 + \alpha|u^n|^2_{1,h}$. Finally, using the Brouwer fixed point theorem, there exists $v^* \in V_h$ such that $\Phi(v^*) = 0$. Taking $u^{n+1} = 2v^* - u^n$, then u^{n+1} satisfies the difference scheme (35). □

The following section is devoted to the study of the stability and convergence of the discretization scheme.

Theorem 4. *Let the weighted parameters $(\lambda_1, \lambda_2, \lambda_3)$ be chosen in set $\mathcal{S}_1^{\mu}(\lambda_1, \lambda_2, \lambda_3)$ or $\mathcal{S}_2^{\mu}(\lambda_1, \lambda_2, \lambda_3)$ or $\mathcal{S}_3^{\mu}(\lambda_1, \lambda_2, \lambda_3)$, and assume that the trigonometric polynomial $Q(\mu, x; \lambda_1, \lambda_2, \lambda_3)$ defined by (31) is non-negative, i.e. $Q(\mu, x; \lambda_1, \lambda_2, \lambda_3) \geq 0$, for all $x \in [-\pi, \pi]$, $0 < \mu < 1$. Then the Crank–Nicolson-WSGD scheme (35) is stable and it follows that*

$$\|u^n\|_h \leq C, \qquad |u^n|_{1,h} \leq C, \qquad \|u^n\|_{\infty,h} \leq C,$$

where C is constant independent on τ and h.

Proof. Taking the discrete L^2 inner product of (35) by multiplying $u^{n+1} + u^n$, we get

$$\begin{aligned}&\frac{1}{\tau}(\|u^{n+1}\|_h - \|u^n\|_h) - \alpha\left(D_tD^2u^n, 2u^{n+\frac{1}{2}}\right)_h + \left(D_0u^n, 2u^{n+\frac{1}{2}}\right)_h\\ &\quad + \left(\mathcal{N}\left(u_j^{n+\frac{1}{2}}\right), u^{n+\frac{1}{2}}\right)_h + \left(\mathcal{D}^{\mu,\lambda_1,\lambda_2,\lambda_3}_{h,1,0,-1}u^{n+\frac{1}{2}}, u^{n+\frac{1}{2}}\right)_h\\ &= \nu\left(D^2u^{n+\frac{1}{2}}, 2u^{n+\frac{1}{2}}\right)_h. &(43)\end{aligned}$$

Noting that (11), we get

$$\left(\mathcal{N}(u), u^{n+\frac{1}{2}}\right)_h = 0. \tag{44}$$

Furthermore, in view of

$$(D_0u^n, 2u^{n+1/2})_h = 0,$$

we have

$$\|u^{n+1}\|_h + \alpha|u^{n+1}|_{1,h} \leq \|u^n\|_h + \alpha|u^n|_{1,h}. \tag{45}$$

It follows Theorem 4 that

$$\|u^n\|_h \leq C, \qquad |u^n|_{1,h} \leq C.$$

Furthermore, using the discrete Sobolev's inequality [38]

$$\|u^n\|_{\infty,h} \leq C_1\|u^n\| + C_2|u|_{1,h},$$

we get

$$\|u^n\|_{\infty,h} \leq C. \quad \square$$

Lemma 7 (*Discrete Gronwall Inequality [38]*)**.** *Suppose $w(k)$, $\varrho(k)$ are non-negative mesh functions and $\varrho(k)$ is non-decreasing. If $C > 0$ and*

$$w(k) \leq \varrho(k) + \tau\sum_{l=0}^{k-1}w(l), \quad \text{for all } k,$$

then we have

$$w(k) \le \varrho(k)\mathrm{e}^{(C\tau k)}, \quad \textit{for all } k. \tag{46}$$

Theorem 5. *Let the weighted parameters $(\lambda_1, \lambda_2, \lambda_3)$ be chosen in set $\mathcal{S}_1^{\mu}(\lambda_1, \lambda_2, \lambda_3)$ or $\mathcal{S}_2^{\mu}(\lambda_1, \lambda_2, \lambda_3)$ or $\mathcal{S}_3^{\mu}(\lambda_1, \lambda_2, \lambda_3)$, and assume that the trigonometric polynomial $Q(\mu, x; \lambda_1, \lambda_2, \lambda_3)$ defined by (31) is non-positive, i.e. $Q(\mu, x; \lambda_1, \lambda_2, \lambda_3) \ge 0$, for all $x \in [-\pi, \pi]$, $0 < \mu < 1$. Let u be the exact solution of problem (2), $\{u^n\}_{n=0}^{J}$ be the solution of (35), then for suitably small τ, we have*

$$\|u(x_j, t_n) - u_j^n\|_{1,h} \le C(\tau^2 + h^2), \quad n \ge 1 \tag{47}$$

where C is a constant independent of T, τ and h.

Proof. Let $e_j^n = v_j^n - u_j^n$, subtracting (35) from (34), we have

$$\begin{aligned} R_j^n = {} & \frac{e_j^{n+1} - e_j^n}{\tau} + D_0 e_j^n - \alpha D_t D^2 e_j^n + (\kappa_{1\,L}\mathcal{D}_{h,1,0,-1}^{\mu,\lambda_1,\lambda_2,\lambda_3} + \kappa_{2\,R}\mathcal{D}_{h,1,0,-1}^{\mu,\lambda_1,\lambda_2,\lambda_3}) e_j^{n+\frac{1}{2}} \\ & + \frac{\delta}{3}\left[v_j^n D_0\left(v_j^{n+\frac{1}{2}}\right) - u_j^n D_0\left(u_j^{n+\frac{1}{2}}\right)\right] + \frac{\delta}{3}\left[D_0\left(v_j^n v_j^{n+\frac{1}{2}}\right) - D_0\left(u_j^n u_j^{n+\frac{1}{2}}\right)\right] - \nu D^2 e_j^{n+\frac{1}{2}}. \end{aligned} \tag{48}$$

For simplicity, we denote

$$I = \frac{\delta}{3}\left[v_j^n D_0\left(v_j^{n+\frac{1}{2}}\right) - u_j^n D_0\left(u_j^{n+\frac{1}{2}}\right)\right], \qquad II = \frac{\delta}{3}\left[D_0\left(v_j^n v_j^{n+\frac{1}{2}}\right) - D_0\left(u_j^n u_j^{n+\frac{1}{2}}\right)\right].$$

Multiplying by $2e_j^{n+\frac{1}{2}}$ on both sides of (48) and summation in j yield

$$\begin{aligned} \frac{1}{\tau}\left(\|e^{n+1}\|_h^2 - \|e^n\|_h^2\right) + \frac{\alpha}{\tau}\left(|e^{n+1}|_{1,h}^2 - |e^n|_{1,h}^2\right) = {} & \left(R^n, e^{n+\frac{1}{2}}\right)_h + \left(\mathcal{D}_{h,1,0,-1}^{\mu,\lambda_1,\lambda_2,\lambda_3} e^{n+\frac{1}{2}}, e^{n+\frac{1}{2}}\right)_h \\ & + \left(I, e^{n+\frac{1}{2}}\right)_h + \left(II, e^{n+\frac{1}{2}}\right)_h + \nu\left(D^2 e^{n+1/2}, e^{n+\frac{1}{2}}\right)_h. \end{aligned} \tag{49}$$

Using Lemma 5, we have

$$\|e^{n+1}\|_h^2 + |e^{n+1}|_{1,h}^2 - \|e^n\|_h^2 - |e^n|_{1,h}^2 \le \tau\left(R^n, e^{n+\frac{1}{2}}\right)_h + \tau\left(I, e^{n+\frac{1}{2}}\right)_h + \tau\left(II, e^{n+\frac{1}{2}}\right)_h.$$

For the first term, using the Cauchy inequality, we get

$$\tau\left(R^n, e^{n+\frac{1}{2}}\right)_h \le \tau\|R^n\|_h^2 + \frac{\tau}{2}\left(\|e^{n+1}\|_h^2 + \|e^n\|_h^2\right). \tag{50}$$

For the second and the third term in (49), we have

$$\left(I, e^{n+\frac{1}{2}}\right)_h \le C\delta\tau\left(|e^{n+1}|_{1,h}^2 + |e^n|_{1,h}^2 + \|e^{n+1}\|_h^2 + \|e^n\|_h^2\right), \tag{51}$$

and

$$\left(II, e^{n+\frac{1}{2}}\right)_h \le \delta C\tau\left(|e^{n+1}|_{1,h}^2 + |e^n|_{1,h}^2 + \|e^{n+1}\|_h^2 + \|e^n\|_h^2\right). \tag{52}$$

In the view of the last term of (49) is non-positive, we obtain

$$\|e^{n+1}\|_{1,h}^2 - \|e^n\|_{1,h}^2 \le C\delta\tau\left(\|e^{n+1}\|_{1,h}^2 + \|e^n\|_{1,h}^2\right) + \tau\|R^n\|_h^2. \tag{53}$$

Moreover, we have

$$(1 - C\delta\tau)(\|e^{n+1}\|_{1,h}^2 - \|e^n\|_{1,h}^2) \le 2C\delta\tau\|e^n\|_{1,h}^2 + \tau\|R^n\|_h^2. \tag{54}$$

In view of for small τ holds $(1 - \tau\delta C) > 0$, we get

$$\|e^{n+1}\|_{1,h}^2 - \|e^n\|_{1,h}^2 \le \|e^n\|_{1,h}^2 + \tau\|R^n\|_h^2. \tag{55}$$

Summation from 0 to $n-1$, for $1 \le n \le N$, shows that

$$\|e^n\|_{1,h}^2 \le \|e^0\|_{1,h}^2 + C\delta\tau\sum_{k=0}^{n-1}\|e^k\|_{1,h}^2 + \tau\sum_{k=0}^{n-1}\|R^k\|_h^2. \tag{56}$$

Table 1
Numerical errors and orders for Example 1 calculated by C–N-WSGL-approximation for different μ in interval $x \in [0, 1]$ and the $(\lambda_1, \lambda_2, \lambda_3)$ are selected in set $\mathcal{S}_1^{\mu}(\lambda_1, \lambda_2, \lambda_3)$ with $\lambda_1 = 0$.

$h = \tau$	$\mu = 0.2$		$\mu = 0.5$		$\mu = 0.8$	
	L^2-error	Order	L^2-error	Order	L^2-error	Order
1/10	5.9620e−04		5.5052e−04		5.0999e−04	
1/20	1.4957e−04	1.9950	1.4009e−04	1.9745	1.3834e−04	1.8822
1/40	3.7432e−05	1.9985	3.5298e−05	1.9887	3.5971e−05	1.9433
1/80	9.3616e−06	1.9994	8.8574e−06	1.9946	9.1677e−06	1.9722

Table 2
Numerical errors and orders for Example 1 calculated by C–N-WSGL-approximation for different μ in interval $x \in [0, 1]$ and the $(\lambda_1, \lambda_2, \lambda_3)$ are selected in set $\mathcal{S}_2^{\mu}(\lambda_1, \lambda_2, \lambda_3)$ with $\lambda_2 = 1.5$.

$h = \tau$	$\mu = 0.2$		$\mu = 0.5$		$\mu = 0.8$	
	L^2-error	Order	L^2-error	Order	L^2-error	Order
1/10	5.2905e−04		4.9576e−04		4.8526e−04	
1/20	1.3335e−04	1.9881	1.2739e−04	1.9604	1.3338e−04	1.8632
1/40	3.3422e−05	1.9964	3.2235e−05	1.9825	3.4893e−05	1.9345
1/80	8.3629e−06	1.9987	8.1048e−06	1.9918	8.9186e−06	1.9680

Note that $R_j^n = O(\tau^2 + h^2)$, we conclude that

$$\|e^n\|_{1,h}^2 \le C(\tau^2 + h^2)^2 + \tau \sum_{k=0}^{n-1} \|e^k\|_{1,h}^2. \tag{57}$$

Combining the above estimation, and using the discrete Gronwall's inequality presented in Lemma 7, we obtain the desired results. □

Remark 2. Many different linearized computational algorithms can be utilized to discrete the nonlinear term uu_x, see [39]. For example, the nonlinear term uu_x can be discreted by the following linearization technique

$$\mathcal{N}(u_j^n) = u_j^n D_0 u_j^{n+1} + u_j^{n+1} D_0 u_j^n. \tag{58}$$

If the approximation to the nonlinear term replaced by formulation (58). We can obtain a new numerical algorithm, we denote it as Crank–Nicolson-WSGD scheme-I, C–N-WSGL-I for short. By the multi-variable Taylor expansion, we can check that the corresponding numerical scheme has second order accuracy in both time and space steps.

5. Numerical results

In this section we investigate numerical examples to show the performance of the proposed new second order C–N-WSGL schemes and confirm the predicted convergence rate. The numerical errors are measured by the discrete L^2 norm defined by (9). We will carry out three numerical examples to illustrate the performance of our numerical methods. The first example is given to show the numerical accuracy for linear Fowler equation presented in Theorem 2. In the next two numerical examples, we numerically evaluate the convergence properties of the proposed methodology aiming at confirming the rates of convergence predicted by the numerical analysis presented in Theorem 5. In following numerical examples, the parameters $\lambda_1, \lambda_2, \lambda_3$ in the trigonometric polynomials $Q(x, \mu; \lambda_1, \lambda_2, \lambda_3)$ satisfy the assumption that presented in Theorems 2 and 5. Without loss of generality, we chose $\kappa_1 = \kappa_2 = 1$ in $\mathcal{D}_x^{\mu}$ (i.e. $\mathcal{D}_x^{\mu} = {}_aD_x^{\mu} + {}_xD_b^{\mu}$) in the first three numerical examples.

Example 1 (*Linear Fowler Equation*)**.** We first consider the following one dimensional problem

$$\begin{aligned} &u_t + u_x + \mathcal{D}_x^{\mu} u = u_{xx} + s(x, t), \quad (x, t) \in (0, 1) \times (0, 1], \\ &u(0, t) = u(1, t) = 0, \quad t \in (0, 1], \\ &u(x, 0) = x^2(1 - x)^2, \quad x \in (0, 1). \end{aligned} \tag{59}$$

Here we take $u(x, t) = \mathrm{e}^{-t}x^2(1 - x)^2$ as the exact solution of (59). And the source term can be determined by simple calculation.

In our computations, the time step is taken as $\tau = h$ in this example. The errors and orders of convergence listed in Tables 1–3 indicate the desired accuracy. Clear second order accuracy for temporal and spatial discretization is observed.

Table 3
Numerical errors and orders for Example 1 calculated by C–N-WSGL-approximation for different μ in interval $x \in [0, 1]$ and the $(\lambda_1, \lambda_2, \lambda_3)$ are selected in set $\mathcal{S}_3^{\mu}(\lambda_1, \lambda_2, \lambda_3)$ with $\lambda_3 = -0.2$.

$h = \tau$	$\mu = 0.2$		$\mu = 0.5$		$\mu = 0.8$	
	L^2-error	Order	L^2-error	Order	L^2-error	Order
1/10	5.6247e−04		5.7269e−04		6.1091e−04	
1/20	1.4144e−04	1.9916	1.4521e−04	1.9796	1.5841e−04	1.9473
1/40	3.5422e−05	1.9974	3.6532e−05	1.9909	4.0323e−05	1.9740
1/80	8.8609e−06	1.9991	9.1606e−06	1.9957	1.0172e−05	1.9870

Table 4
Numerical errors and orders for Example 2 calculated by C–N-WSGL and C–N-WSGL-I schemes for different μ in interval $x \in [0, 1]$ and the $(\lambda_1, \lambda_2, \lambda_3)$ are selected in set $\mathcal{S}_1^{\mu}(\lambda_1, \lambda_2, \lambda_3)$ with $\lambda_1 = 0$.

Scheme	$h = \tau$	$\mu = 0.1$		$\mu = 0.5$		$\mu = 0.9$	
		L^2-error	Order	L^2-error	Order	L^2-error	Order
C–N-WSGL	1/10	5.9676e−04		5.3687e−04		4.9044e−04	
	1/20	1.5017e−04	1.9905	1.3736e−04	1.9666	1.4121e−04	1.7962
	1/40	4.0377e−05	1.8950	3.7515e−05	1.8724	4.0570e−05	1.7994
C–N-WSGL-I	1/10	5.9654e−04		5.3664e−04		4.9018e−04	
	1/20	1.4935e−04	1.9979	1.3652e−04	1.9748	1.4032e−04	1.8046
	1/40	3.7353e−05	1.9994	3.4404e−05	1.9884	3.7434e−05	1.9063

Table 5
Numerical errors and orders for Example 2 calculated by C–N-WSGL and C–N-WSGL-I schemes for different μ in interval $x \in [0, 1]$ and the $(\lambda_1, \lambda_2, \lambda_3)$ are selected in set $\mathcal{S}_2^{\mu}(\lambda_1, \lambda_2, \lambda_3)$ with $\lambda_2 = 1.5$.

Scheme	$h = \tau$	$\mu = 0.1$		$\mu = 0.5$		$\mu = 0.9$	
		L^2-error	Order	L^2-error	Order	L^2-error	Order
C–N-WSGL	1/10	5.2763e−04		4.8055e−04		4.7781e−04	
	1/20	1.3346e−04	1.9832	1.2434e−04	1.9504	1.3899e−04	1.7815
	1/40	3.6550e−05	1.8684	3.4633e−05	1.8440	4.0171e−05	1.7907
C–N-WSGL-I	1/10	5.2738e−04		4.8029e−04		4.7753e−04	
	1/20	1.3254e−04	1.9924	1.2341e−04	1.9605	1.3808e−04	1.7901
	1/40	3.3181e−05	1.9980	3.1238e−05	1.9820	3.7001e−05	1.8999

Table 6
Numerical errors and orders for Example 2 calculated by C–N-WSGL and C–N-WSGL-I schemes for different μ in interval $x \in [0, 1]$ and the $(\lambda_1, \lambda_2, \lambda_3)$ are selected in set $\mathcal{S}_3^{\mu}(\lambda_1, \lambda_2, \lambda_3)$ with $\lambda_3 = -0.2$.

Scheme	$h = \tau$	$\mu = 0.1$		$\mu = 0.5$		$\mu = 0.9$	
		L^2-error	Order	L^2-error	Order	L^2-error	Order
C–N-WSGL	1/10	5.5055e−04		5.5963e−04		6.1904e−04	
	1/20	1.3901e−04	1.9857	1.4261e−04	1.9724	1.6363e−04	1.9196
	1/40	3.7815e−05	1.8781	3.8687e−05	1.8822	4.4614e−05	1.8749
C–N-WSGL-I	1/10	5.5032e−04		5.5941e−04		6.1883e−04	
	1/20	1.3813e−04	1.9942	1.4180e−04	1.9800	1.6286e−05	1.9260
	1/40	3.4568e−05	1.9985	3.5678e−05	1.9908	4.1779e−05	1.9628

Example 2 (*Nonlinear Fowler Equation*)**.** We next consider the following one dimensional problem

$$\begin{aligned} &u_t + uu_x + \mathcal{D}_x^{\mu} u = u_{xx} + s(x, t), \quad (x, t) \in (0, 1) \times (0, 1], \\ &u(0, t) = u(1, t) = 0, \quad t \in (0, 1], \\ &u(x, 0) = x^2(1 - x)^2, \quad x \in (0, 1). \end{aligned} \tag{60}$$

Taking $u(x, t) = \mathrm{e}^{-t}x^2(1 - x)^2$ as the exact solution of (60). We can get the source term with the help of the formulae of the fractional derivatives [1].

By examining the numerical errors with mesh refinements, the numerically calculated orders of convergence are listed in Tables 4–6. We note that the accuracies and orders of the C–N-WSGL and C–N-WSGL-I schemes are almost identical, while the orders of the proposed C–N-WSGL-I scheme are slightly higher on the dense meshes.

Table 7
Numerical errors and orders for Example 3 calculated by C–N-WSGL and C–N-WSGL-I schemes for different μ in interval $x \in [0, 1]$ and the $(\lambda_1, \lambda_2, \lambda_3)$ are selected in set $\mathcal{S}_1^{\mu}(\lambda_1, \lambda_2, \lambda_3)$ with $\lambda_1 = 0$.

Scheme	$h = \tau$	$\mu = 0.3$		$\mu = 0.5$		$\mu = 0.7$	
		L^2-error	Order	L^2-error	Order	L^2-error	Order
C–N-WSGL	1/10	1.3880e−04		1.4927e−04		1.6708e−04	
	1/20	3.4498e−05	2.0084	3.6575e−05	2.0290	3.9642e−05	2.0754
	1/40	9.4664e−06	1.8656	9.8612e−06	1.8910	1.0398e−05	1.9307
C–N-WSGL-I	1/10	1.3809e−04		1.4864e−04		1.6654e−04	
	1/20	3.3678e−05	2.0358	3.5830e−05	2.0526	3.8967e−05	2.0955
	1/40	8.3584e−06	2.0105	8.8321e−06	2.0204	9.4332e−06	2.0464

Table 8
Numerical errors and orders for Example 3 calculated by C–N-WSGL and C–N-WSGL-I schemes for different μ in interval $x \in [0, 1]$ and the $(\lambda_1, \lambda_2, \lambda_3)$ are selected in set $\mathcal{S}_2^{\mu}(\lambda_1, \lambda_2, \lambda_3)$ with $\lambda_2 = 1.5$.

Scheme	$h = \tau$	$\mu = 0.3$		$\mu = 0.5$		$\mu = 0.7$	
		L^2-error	Order	L^2-error	Order	L^2-error	Order
C–N-WSGL	1/10	1.5651e−04		1.6527e−04		1.7817e−04	
	1/20	3.8584e−05	2.0202	4.0175e−05	2.0404	4.1960e−05	2.0861
	1/40	1.0354e−05	1.8978	1.0635e−05	1.9175	1.0873e−05	1.9482
C–N-WSGL-I	1/10	1.5593e−04		1.6474e−04		1.7769e−04	
	1/20	3.7888e−05	2.0410	3.9525e−05	2.0593	4.1339e−05	2.1037
	1/40	9.3877e−06	2.0129	9.7149e−06	2.0245	9.9689e−06	2.0520

Table 9
Numerical errors and orders for Example 3 calculated by C–N-WSGL and C–N-WSGL-I schemes for different μ in interval $x \in [0, 1]$ and the $(\lambda_1, \lambda_2, \lambda_3)$ are selected in set $\mathcal{S}_3^{\mu}(\lambda_1, \lambda_2, \lambda_3)$ with $\lambda_3 = -0.2$.

Scheme	$h = \tau$	$\mu = 0.3$		$\mu = 0.5$		$\mu = 0.7$	
		L^2-error	Order	L^2-error	Order	L^2-error	Order
C–N-WSGL	1/10	1.4370e−04		1.4311e−04		1.4561e−04	
	1/20	3.5615e−05	2.0125	3.5212e−05	2.0230	3.5230e−05	2.0472
	1/40	9.7059e−06	1.8755	9.5735e−06	1.8790	9.5127e−06	1.8889
C–N-WSGL-I	1/10	1.4303e−04		1.4245e−04		1.4495e−04	
	1/20	3.4832e−05	2.0378	3.4425e−05	2.0489	3.4434e−05	2.0737
	1/40	8.6398e−06	2.0113	8.4976e−06	2.0183	8.4144e−06	2.0329

Example 3 (*Fractional Kakutani–Matsuuchi Equation*)**.** We next consider the following one dimensional problem

$$\begin{aligned} &u_t + u_x - u_{txx} + \mathcal{D}_x^{\mu} u + uu_x = s(x, t), \quad (x, t) \in (0, 1) \times (0, 1], \\ &u(0, t) = u(1, t) = 0, \quad t \in (0, 1], \\ &u(x, 0) = x^3(1 - x)^3, \quad x \in (0, 1). \end{aligned} \tag{61}$$

Taking $u(x, t) = \mathrm{e}^{-t}x^3(1 - x)^3$ as the exact solution of (61). The source term $s(x, t)$ can be obtained by the exact solution.

The discrete L^2 errors is given in Tables 7–10. From Tables 7–10, we see that the numerical solutions converge to the theoretical solution in the L^2 norm. The proposed numerical schemes are both unconditionally stable. And the numerical results presented in Tables 7–10 are in good agreement with our theoretical analysis predicted in Theorem 5.

Form numerical results presented in Examples 2 and 3, we see that the C–N-WSGL-I scheme performs better in the computation, while the C–N-WSGL scheme is more convenient for error analysis. It reveals that the C–N-WSGL-I scheme is more accurate than the C–N-WSGL scheme. And the second order of convergence for the C–N-WSGL scheme will be reduced when the mesh size is truly small. This is due to the different treatment of the nonlinear term uu_x.

Example 4 (*Effect of Parameters*)**.** In this example, we study the influence of the different parameters in Eq. (1). More specifically, we consider the following problem

$$u_t + u_x - \alpha u_{txx} + \mathcal{D}_x^{\mu} u + \delta uu_x = 0, \quad (x, t) \in (0, T) \times (0, L], \tag{62}$$

with the initial data

$$u_0(x) = 0.32\,\mathrm{sech}^2(0.4(x - x_0)).$$

Here, the $\mathcal{D}_x^{\mu} = \left[\kappa_1\, {}_aD_x^{\mu} + \kappa_2\, {}_xD_b^{\mu}\right]$ is fractional derivative operator defined by (5).

Table 10
Numerical errors and orders for Example 3 calculated by C–N-WSGL and C–N-WSGL-I schemes at different time t in interval $x \in [0, 1]$ and the $(\lambda_1, \lambda_2, \lambda_3)$ are selected in set $\mathcal{S}_3^{\mu}(\lambda_1, \lambda_2, \lambda_3)$ with $\lambda_3 = -0.2$ and $\mu = 0.5$.

Scheme	$h = \tau$	$t = 10$		$t = 15$		$t = 20$	
		L^2-error	Order	L^2-error	Order	L^2-error	Order
C–N-WSGL	1/10	1.5694e−04		1.1755e−04		7.2288e−05	
	1/20	4.3726e−05	1.8437	3.3235e−05	1.8225	2.0555e−05	1.8142
	1/40	1.1752e−05	1.8956	8.5549e−06	1.9579	5.0519e−06	2.0246
C–N-WSGL-I	1/10	1.5631e−04		1.1750e−04		7.2534e−05	
	1/20	4.3022e−05	1.8612	3.3229e−05	1.8221	2.0889e−05	1.7959
	1/40	1.0975e−05	1.9709	8.5308e−06	1.9617	5.3810e−06	1.9568

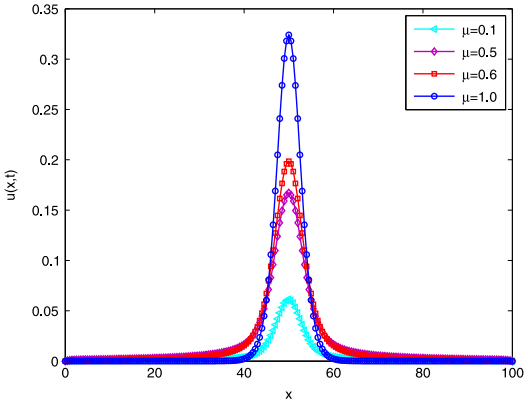

Fig. 4. Numerical solutions with the different μ at time $T = 1$, where $\kappa_1 = \kappa_2 = 1.0$, $\alpha = \delta = 1$.

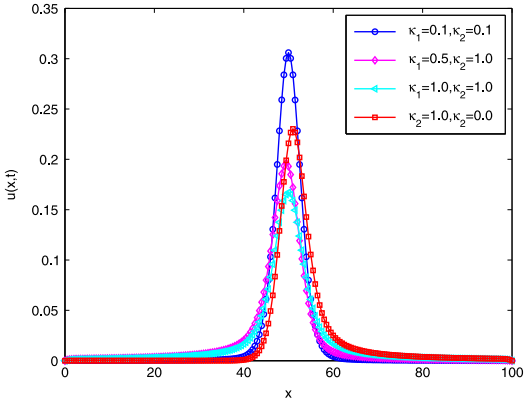

Fig. 5. Numerical solutions with the different viscosity κ_1, κ_2, and $\alpha = \delta = 1$ at time $T = 1$.

In all the computations presented below, we use the C–N-WSGL scheme with $\tau = h = 1/2$, and the parameters $(\lambda_1, \lambda_2, \lambda_3)$ are selected in set $\mathcal{S}_1^{\mu}(\lambda_1, \lambda_2, \lambda_3)$ with $\lambda_1 = 0$. The length of interval gives $L = 100$, and the middle of the interval gives $x_0 = 50$. The numerical simulations are plotted in Figs. 4–6. The numerical simulations results show that the nonlocal viscous term provides dissipation.

Influence of parameter μ in (62) with $\kappa_1 = \kappa_2 = 1.0$, $\alpha = \delta = 1$ at time $T = 1$ are presented in Fig. 4. From this figure we can see that the dissipation of μ plays more important role. Fig. 5 shows the effect of varying the skewness coefficient of κ_1 and κ_2. The evolution of numerical solutions is shown in Fig. 6. The simulation results are consistent with the analysis given in Refs. [40–42].

6. Conclusion

In this paper, we have constructed and investigated a set of second-order accurate and efficient numerical methods for a water wave model with nonlocal viscous dispersive term. The convergence analysis has been carried out for the presented schemes. Our theoretical analysis shown that the presented schemes are unconditionally stable with second-order accurate. Finally, the numerical and simulation results demonstrated the designed second order accuracy and performance of the

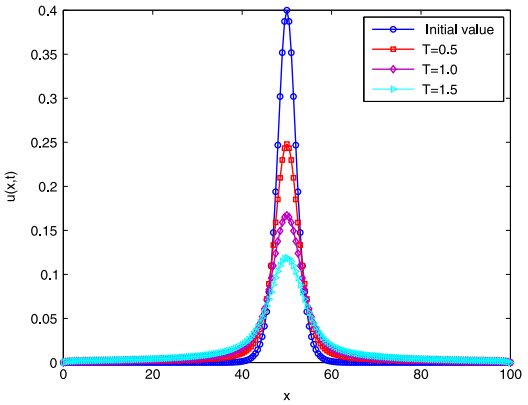

Fig. 6. Numerical solutions with $\kappa_1 = \kappa_2 = 1.0$, $\mu = 0.5$, $\alpha = \delta = 1$ at different times.

schemes constructed in this paper. In fact, with the help of the techniques presented in [43], our algorithms can also be used to solve the considered models with nonhomogeneous boundary conditions. We expect that the numerical schemes presented here may be helpful to understand the dissipation behavior of the water wave models.

Acknowledgments

The authors thank the anonymous referees for their valuable comments and suggestions on a previous version of this paper. C. Li would like to thank Martin Stynes for his very helpful comments and suggestions. This research was partially supported by the National Natural Science Foundation of China under Grant Nos. 11271173, 11426174 and 51305344, the Starting Research Fund from the Xi'an university of Technology under Grant Nos. 108-211206, 2014CX022 and the Natural Science Basic Research Plan in Shaanxi Province of China under Grant No. 2015JQ1022.

References

[1] I. Podlubny, Fractional Differential Equations, Academic Press, San Diego, 1999.
[2] S. Samko, A. Kilbas, O. Marichev, Fractional Integrals and Derivatives: Theory and Applications, Gordon and Breach, London, 1993.
[3] W. Chen, S. Holm, Fractional Laplacian time–space models for linear and nonlinear lossy media exhibiting arbitrary frequency dependency, J. Acoust. Soc. Am. 115 (2004) 1424–1430.
[4] J.L. Bona, K. Promislow, C.E. Wayne, Higher-order asymptotics of decaying solutions of some nonlinear, dispersive, dissipative wave equations, Nonlinearity 8 (1995) 1179–1206.
[5] M. Chen, S. Dumont, O. Goubet, Decay of solutions to a viscous asymptotical model for water waves: Kakutani–Matsuuchi model, Nonlinear Anal.: Theory Methods Appl. 75 (2012) 2883–2896.
[6] T. Kakutani, M. Matsuuchi, Effect of viscosity of long gravity waves, J. Phys. Soc. Japan 39 (1975) 237–246.
[7] N. Alibaud, P. Azerad, D. Isèbe, A non-monotone conservation law for dune morphodynamics, Differential Integral Equations 23 (2010) 155–188.
[8] P. Azerad, A. Bouharguane, J. Crouzet, Simultaneous denoising and enhancement of signals by a fractal conservation law, Commun. Nonlinear Sci. Numer. Simul. 17 (2012) 867–881.
[9] G.I. Jennings, Efficient numerical methods for water wave propagation in unbounded domains (Ph.D. thesis), Applied and Interdisciplinary Mathematics, The University of Michigan, 2012.
[10] J. Droniou, A numerical method for fractal conservation laws, Math. Comp. 76 (2010) 95–124.
[11] F. Achleitner, S. Hittmeir, C. Schmeiser, On nonlinear conservation laws with a nonlocal diffusion term, J. Differential Equations 250 (2011) 2177–2196.
[12] Q. Du, M. Gunzburger, R.B. Lehoucq, K. Zhou, Analysis and approximation of nonlocal diffusion problems with volume constraints, SIAM Rev. 56 (2012) 676–696.
[13] Q. Du, J.R. Kamm, R.B. Lehoucq, M.L. Parks, A new approach for a nonlocal, nonlinear conservation law, SIAM J. Appl. Math. 72 (2012) 464–487.
[14] B. Jourdain, R. Roux, Convergence of a stochastic particle approximation for fractional scalar conservation laws, Stochastic Process. Appl. 121 (2011) 957–988.
[15] M.M. Meerschaert, C. Tadjeran, Finite difference approximations for fractional advection–dispersion flow equations, J. Comput. Appl. Math. 172 (2004) 65–77.
[16] M.M. Meerschaert, C. Tadjeran, Finite difference approximations for two-sided space-fractional partial differential equations, Appl. Numer. Math. 56 (2006) 80–90.
[17] E. Sousa, Finite difference approximations for a fractional advection diffusion problem, J. Comput. Phys. 228 (2009) 4038–4054.
[18] W.Y. Tian, H. Zhou, W.H. Deng, A class of second order difference approximations for solving space fractional diffusion equations, Math. Comp. 84 (2015) 1703–1727.
[19] W.H. Deng, J.S. Hesthaven, Local discontinuous Galerkin methods for fractional diffusion equations, ESAIM: Math. Model. Numer. Anal. 47 (2013) 1845–1864.
[20] F.W. Liu, V. Anh, I. Turner, Numerical solution of the space fractional Fokker–Planck equation, J. Comput. Appl. Math. 166 (2004) 209–219.
[21] Z. Wang, S. Vong, Compact difference schemes for the modified anomalous fractional sub-diffusion equation and the fractional diffusion-wave equation, J. Comput. Phys. 277 (2013) 1–15.
[22] C.P. Li, F.H. Zeng, Finite difference methods for fractional differential equations, Internat. J. Bifur. Chaos 22 (2012) 1230014.
[23] Z.Z. Sun, X.N. Wu, A fully discrete difference scheme for a diffusion-wave system, Appl. Numer. Math. 56 (2006) 193–209.
[24] Z. Fu, W. Chen, H. Yang, Boundary particle method for Laplace transformed time fractional diffusion equations, J. Comput. Phys. 235 (2012) 52–66.
[25] H. Wang, N. Du, A superfast-preconditioned iterative method for steady-state space-fractional diffusion equations, J. Comput. Phys. 240 (2013) 49–57.
[26] Q. Yang, F. Liu, I. Turner, Numerical methods for fractional partial differential equations with Riesz space fractional derivatives, Appl. Math. Model. 34 (2010) 200–218.

[27] P. Biler, T. Funaki, W.A. Woyczyński, Interacting particle approximation for nonlocal quadratic evolution problems, Probab. Math. Statist. 19 (1999) 267–286.
[28] V.J. Ervin, N. Heuer, J.P. Roop, Numerical approximation of a time dependent, nonlinear, space-fractional diffusion equation, SIAM J. Numer. Anal. 45 (2007) 572–591.
[29] S. Cifani, E.R. Jakobsen, K.H. Karlsen, The discontinuous Galerkin method for fractal conservation laws, IMA J. Numer. Anal. 31 (2011) 1090–1122.
[30] Q.W. Xu, J.S. Hesthaven, Discontinuous Galerkin methods for fractional convection diffusion equations, SIAM J. Numer. Anal. 52 (2014) 405–423.
[31] Z. Mao, J. Shen, A semi-implicit spectral deferred correction method for two water wave models with nonlocal viscous term and numerical study of their decay rates, Sci. China Math. 8 (2015) 1153–1168.
[32] G.Y. Xue, L.M. Zhang, A new finite difference scheme for generalized Rosenau–Burgers equation, Appl. Math. Comput. 222 (2013) 490–496.
[33] C. Li, W.H. Deng, Second order WSGD operators II: A new family of second order difference approximations for solving space fractional advection diffusion equations, 2013. arXiv:1310.7671 [math.NA].
[34] A. Quarteroni, R. Sacco, F. Saleri, Numerical Mathematics, second ed., Springer, 2007.
[35] R.H. Chan, Toeplitz preconditioners for Toeplitz systems with nonnegative generating functions, IMA J. Numer. Anal. 11 (1991) 333–345.
[36] G.H. Golub, C.F. Van Loan, Matrix Computations, third ed., The Johns Hopkins University Press, 1996.
[37] F.E. Browder, Existence and uniqueness theorems for solutions of nonlinear boundary value problems, Proc. Sympos. Appl. Math. 17 (1965) 24–49.
[38] Y. Zhou, Application of Discrete Functional Analysis to the Finite Difference Method, International Academy Publishers, Beijing, 1990.
[39] C.A.J. Fletcher, Computational Techniques for Fluid Dynamics, Vol. I and II, in: Springer Series in Computational Physics, Springer, 1988.
[40] A.S. Chaves, A fractional diffusion equation to describe Lévy flights, Phys. Lett. A 239 (1998) 13–16.
[41] D.A. Benson, S.W. Wheatcraft, M.M. Meerschaert, The fractional-order governing equation of Lévy motion, Water Resour. Res. 36 (2000) 1413–1423.
[42] R. Metzler, J. Klafter, The random walk's guide to anomalous diffusion: A fractional dynamics approach, Phys. Rep. 339 (2000) 1–77.
[43] L. Zhao, W.H. Deng, A series of high-order quasi-compact schemes for space fractional diffusion equations based on the superconvergent approximations for fractional derivatives, Numer. Methods Partial Differential Equations 31 (2015) 1345–1381.